Ching-Shin Norman Shiau
Postdoctoral Research Fellow
e-mail: cshiau@alumni.cmu.edu

Nikhil Kaushal
Research Assistant
e-mail: nkaushal@alumni.cmu.edu

Mechanical Engineering,
Carnegie Mellon University,
Pittsburgh, PA 15213

Chris T. Hendrickson
Professor
Civil and Environmental Engineering,
Carnegie Mellon University,
Pittsburgh, PA 15213
e-mail: cth@cmu.edu

Scott B. Peterson
Research Assistant
Engineering and Public Policy,
Carnegie Mellon University,
Pittsburgh, PA 15213
e-mail: speterson@cmu.edu

Jay F. Whitacre
Assistant Professor
Engineering and Public Policy,
and Materials Science and Engineering,
Carnegie Mellon University,
Pittsburgh, PA 15213
e-mail: whitacre@andrew.cmu.edu

Jeremy J. Michalek[1]
Associate Professor
Mechanical Engineering,
and Engineering and Public Policy,
Carnegie Mellon University,
Pittsburgh, PA 15213
e-mail: jmichalek@cmu.edu

Optimal Plug-In Hybrid Electric Vehicle Design and Allocation for Minimum Life Cycle Cost, Petroleum Consumption, and Greenhouse Gas Emissions

Plug-in hybrid electric vehicle (PHEV) technology has the potential to reduce operating cost, greenhouse gas (GHG) emissions, and petroleum consumption in the transportation sector. However, the net effects of PHEVs depend critically on vehicle design, battery technology, and charging frequency. To examine these implications, we develop an optimization model integrating vehicle physics simulation, battery degradation data, and U.S. driving data. The model identifies optimal vehicle designs and allocation of vehicles to drivers for minimum net life cycle cost, GHG emissions, and petroleum consumption under a range of scenarios. We compare conventional and hybrid electric vehicles (HEVs) to PHEVs with equivalent size and performance (similar to a Toyota Prius) under urban driving conditions. We find that while PHEVs with large battery packs minimize petroleum consumption, a mix of PHEVs with packs sized for ~25–50 miles of electric travel under the average U.S. grid mix (or ~35–60 miles under decarbonized grid scenarios) produces the greatest reduction in life cycle GHG emissions. Life cycle cost and GHG emissions are minimized using high battery swing and replacing batteries as needed, rather than designing underutilized capacity into the vehicle with corresponding production, weight, and cost implications. At 2008 average U.S. energy prices, Li-ion battery pack costs must fall below $590/kW h at a 5% discount rate or below $410/kW h at a 10% rate for PHEVs to be cost competitive with HEVs. Carbon allowance prices offer little leverage for improving cost competitiveness of PHEVs. PHEV life cycle costs must fall to within a few percent of HEVs in order to offer a cost-effective approach to GHG reduction. [DOI: 10.1115/1.4002194]

Keywords: plug-in hybrid electric vehicle, greenhouse gas emissions, environmental policy, design optimization, mixed-integer nonlinear programming, battery degradation, vehicle design

1 Introduction

Plug-in hybrid electric vehicle (PHEV) technology is considered a potential near-term approach to addressing global warming and U.S. dependency on foreign oil in the transportation sector as the cost, size, and weight of batteries are reduced [1]. PHEVs use large battery packs to store energy from the electricity grid and propel the vehicle partly on electricity instead of gasoline. Under the average mix of electricity sources in the U.S., vehicles can be driven with lower operation cost and fewer greenhouse gas (GHG) emissions per mile when powered by electricity rather than by gasoline [2]. PHEVs have the potential to displace a large portion of the gasoline consumed by the transportation sector with electricity since approximately 60% of U.S. passenger vehicles travel less than 30 miles each day [3]. Several automobile manufacturers have announced plans to produce PHEVs commercially in the future, including General Motors' Chevrolet Volt, which will carry enough battery modules to store 40 miles worth of electricity [4] and Toyota's plug-in version of the Prius, which will carry enough batteries for approximately 13 miles of electric travel [5].

The structure of a PHEV is similar to that of an ordinary hybrid electrical vehicle (HEV), except that the PHEV carries a larger battery pack and offers plug-charging capability [6]. PHEVs store energy from the electricity grid to partially offset gasoline use for propulsion. The hybrid drivetrain has several advantages in terms of improving vehicle efficiency. First, the electric motor enables the engine to operate at its most efficient load most of the time, utilizing the batteries to smooth out spikes in power demand. Second, having an additional source of power in the form of an electric motor enables designers to select smaller engine designs with higher fuel efficiency and lower torque capabilities. Third, HEV and PHEV powertrains enable energy that is otherwise lost in braking to be captured to charge the battery and enable the engine to be shut off rather than idling when the vehicle is at rest.

We focus on the split configuration in our PHEV study because of its flexibility to operate similarly to a parallel or series driv-

[1]Corresponding author.

Contributed by the Design Engineering Committee of ASME for publication in the JOURNAL OF MECHANICAL DESIGN. Manuscript received December 20, 2009; final manuscript received July 15, 2010; published online September 20, 2010. Guest Editor: Steven J. Skerlos.

 Copyright © 2010 by ASME

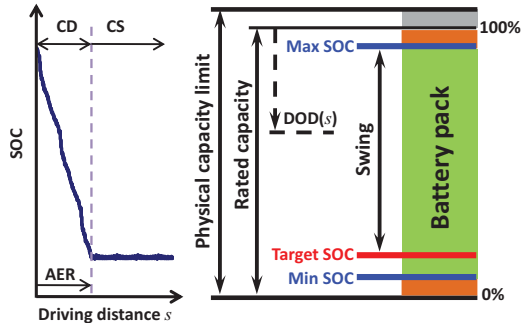

Fig. 1 Battery state of charge characteristics

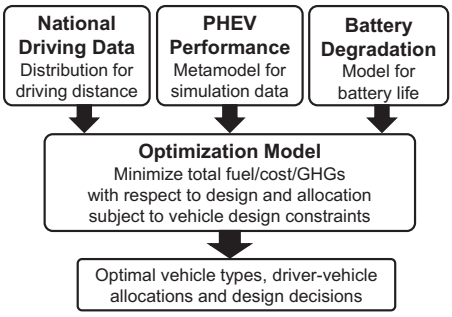

Fig. 2 Framework of optimal PHEV design and allocation

etrain [6,7], and we adopt an all-electric control strategy,[2] which disables engine operation in charge-depleting (CD) mode and draws propulsion energy entirely from the battery until it reaches a target state of charge (SOC), as shown in Fig. 1. The distance that a PHEV can travel on electricity alone with a fully charged battery is called its all-electric range (AER).[3] Once the driving distance reaches the AER and the battery is depleted to the target SOC, the PHEV switches to operate in charge-sustaining (CS) mode, and the gasoline engine provides energy to propel the vehicle and maintain battery charge near the target SOC. In CS mode, the PHEV operates similarly to an ordinary HEV.

The battery diagram in Fig. 1 presents several definitions relevant to battery capacity. Each cell's physical capacity limit may vary, and charging past physical capacity limits is dangerous, so the 100% rated capacity is set below the physical limit. Maximum, target, and minimum SOC are further determined by hybrid vehicle designers based on their design application. We define the capacity window between maximum and target SOC as SOC swing and the ratio of discharged capacity to the rated capacity as depth of discharge (DOD), where DOD is a function of driving distance s. We further define *state of energy* (SOE) as the percent of energy remaining in the battery: SOE=energy remaining/energy capacity. If the battery voltage is constant with SOC, then SOC and SOE are equivalent; we use SOE and the corresponding *battery energy swing* to focus on the quantity of interest throughout the study.

Generally, increased AER will result in a larger portion of travel propelled by electrical energy instead of gasoline; however, the distance the vehicle is driven between charges plays an important role in determining the PHEV's advantage: Vehicles that are charged frequently can drive most of their miles on electric power, even with a relatively small battery pack, while vehicles that are charged infrequently require larger battery packs to cover longer distances with electric power [9].

Battery degradation and replacement also affect PHEV implications. Modern batteries have limited life, and frequent cycling leads to accelerated degradation, including reduction in battery capacity and increase in internal resistance caused by the growth of a solid-electrolyte interphase (SEI) layer and a solid film layer on the electrode during battery storage and cycling [10]. A commonly used model of battery degradation views degradation as an increasing function of DOD [11–14], implying that designers should avoid cycling batteries to a deep DOD. However, Peterson et al. [15] used realistic driving cycles to demonstrate that modern $LiFePO_4$ batteries degrade as a function of energy processed, irrespective of DOD, which has implications for PHEV design.[4]

2 Model

We pose a benevolent dictator optimization model to determine optimal vehicle type, design, and allocation for achieving social objectives of minimum equivalent daily cost, life cycle GHG emissions, and petroleum consumption from personal transportation.[5] Figure 2 shows an overview of the modeling framework. For the single vehicle case, the objective function can be expressed as the integral of the corresponding quantity per day at each driving distance $f_O(\mathbf{x},s)$ times the probability distribution of daily driving distances $f_S(s)$ in the population of drivers:

$$\underset{\mathbf{x}}{\text{minimize}} \int_0^\infty f_O(\mathbf{x},s) f_S(s) ds$$

$$\text{subject to } \mathbf{g}(\mathbf{x}) \le \mathbf{0}, \quad \mathbf{h}(\mathbf{x}) = \mathbf{0} \tag{1}$$

where $\mathbf{x}$ is a vector of design variables that define the vehicle, s is the distance the vehicle is driven between charges, $f_O(\mathbf{x},s)$ is the value of the objective (equivalent cost, petroleum consumption, or GHG emissions) per day for vehicle design $\mathbf{x}$ when driven s miles/day, $f_S(s)$ is the probability density function for the distance driven per day, $\mathbf{g}(\mathbf{x})$ is a vector of inequality constraints, and $\mathbf{h}(\mathbf{x})$ is a vector of equality constraints ensuring a feasible vehicle design. We assume that each vehicle is charged once per day, so that s indicates the distance traveled between charges.

To extend this model to the case where different drivers are assigned different vehicles based on the distance driven per day, we incorporate a new decision variable s_i that defines the cutoff point such that drivers who travel less than s_i per day are assigned the vehicle defined by $\mathbf{x}_i$ and drivers who travel more than s_i per day are assigned the vehicle defined by $\mathbf{x}_{i+1}$. Extending this idea to n segments, the formulation for vehicle design and ordered allocation is given by

$$\underset{\mathbf{x}_i, s_i \forall i \in \{1,\ldots,n\}}{\text{minimize}} \sum_{i=1}^{n} \left(\int_{s_{i-1}}^{s_i} f_O(\mathbf{x}_i,s) f_S(s) ds \right)$$

$$\text{subject to } \mathbf{g}(\mathbf{x}_i) \le \mathbf{0}, \quad \mathbf{h}(\mathbf{x}_i) = \mathbf{0}, \quad \forall\, i \in \{1,\ldots,n\}$$

$$s_i \ge s_{i-1}, \quad \forall\, i \in \{1,\ldots,n\}$$

$$\text{where } s_0 = 0, \quad s_n = \infty \tag{2}$$

Taking a two-segment case as an example, the vehicle 1 segment contains vehicles that travel between $[0, s_1]$ miles/day, the vehicle 2 segment contains vehicles that travel between $[s_1, \infty]$

[2] A blended-strategy PHEV uses a mix of the electric motor and gasoline engine to power the vehicle in CD mode. We confine our scope to the all-electric strategy for simplicity since blended-strategy operation characteristics are sensitive to control parameters.

[3] AER is defined as energy-equivalent electric propulsion distance for blended-mode PHEVs, but we consider only all-electric PHEVs in this study [8].

[4] This pattern was also observed experimentally by [16].

[5] We model allocation of vehicles to drivers as a dictated assignment based on driver daily travel distance and do not model market mechanisms or consumer choice [17,18]. As such, we find the best possible outcome for reducing petroleum consumption, life cycle cost, or GHG emissions, which is a lower bound for market-based outcomes.

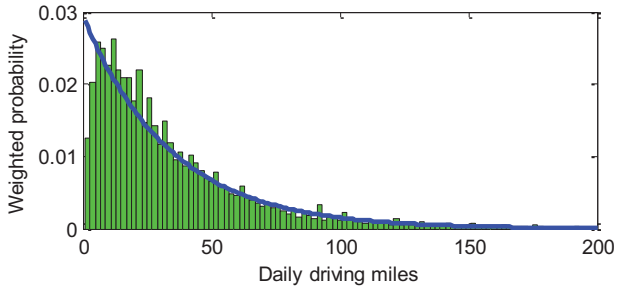

Fig. 3 Probability density function for vehicle miles traveled per day

miles/day, and the optimal value of s_1 is determined together with the vehicle design variable vectors $\mathbf{x}_1$ and $\mathbf{x}_2$ for vehicles 1 and 2.

In the following subsections, we first instantiate this formulation with specific models for the objective and constraint functions by specifying the distribution of distance driven per day, vehicle performance models, battery degradation models, and the objective and constraint functions.

2.1 Distribution of Vehicle Miles Traveled per Day. We use data from the 2009 National Household Transportation Survey (NHTS) [19] to estimate the distribution of distance driven per day over the population of drivers. The survey collected data by interviewing 136,410 households across the U.S. on the mode of transportation, duration, distance, and purpose of the trips taken on the survey day. We fit the weighted driving data using the exponential distribution.[6] The distribution below represents the probability density function for vehicle miles traveled by drivers on the day surveyed:

$$f_S(s) = \lambda e^{-\lambda s}, \quad s \geq 0 \tag{3}$$

The coefficient λ is 0.0296 estimated using the maximum likelihood method. Figure 3 shows the exponential distribution and the histogram of the surveyed daily vehicle driving miles.[7] Because we lack multiple days of data for each vehicle, we assume that a vehicle that travels s miles/day on the NHTS survey day will travel s miles every day. This assumption will produce optimistic results on the benefits of optimal allocation since distance traveled varies over time for individual vehicles in practice.

2.2 Vehicle Performance Models. We carry out vehicle performance simulations using the Powertrain Systems Analysis Toolkit (PSAT) 6.2 SP1 vehicle physics simulator developed by Argonne National Laboratory [20]. PSAT is a MATLAB/SIMULINK forward-looking simulation package that predicts vehicle performance characteristics at both the system level (e.g., fuel consumption) and the component level (e.g., engine torque and speed at each time step) over a given driving cycle using a combination of first principles and empirical component data. In our study, the body, powertrain, and vehicle parameters for all PHEV and HEV simulations are based on the 2004 Toyota Prius model that uses the split powertrain system with an Atkinson engine, a permanent magnet motor, and a nickel-metal hydride (NiMH) battery pack. To account for structural weight needed to carry heavy battery packs, we include an additional 1 kg of structural weight per 1 kg of battery and motor weight [9]. We created a comparable conventional vehicle (CV) model using a conventional powertrain and four-cylinder engine based on the Honda Accord to account for larger engine torque and power requirements, and the parameters that define the frontal area, drag coefficient, and base weight are adjusted to match the Prius for a fair comparison. The vehicle configuration parameters are included in Table 2 in the Appendix.

For the PHEV design, the Prius engine size is scaled by the peak power output from the base engine (57 kW) using linear scaling. Similarly, the motor is scaled from the base motor (52 kW) linearly. Both the engine and motor weights are also scaled proportionally to the peak power. We use the Saft Li-ion battery module in the PSAT package for the PHEV energy storage device. Each cell in the module weighs 0.378 kg, with a modified specific energy of 100 W h/kg, an energy capacity of 21.6 W h, and a nominal output voltage of 3.6 V. The weight of each three-cell module is 1.42 kg using a packaging factor of 1.25. The battery size and capacity are scaled by specifying the number of cells in the pack. We use a split control strategy modified for a PHEV target SOC, and we assume an 800 W base electrical hotel load for all vehicles. We use the U.S. Environmental Protection Agency's Urban Dynamometer Driving Schedule (UDDS) driving cycle [21] to calculate simulated electrical efficiency (miles/kW h) in CD mode for PHEVs, and gasoline efficiency (mpg) in CS mode for all vehicles.[8] We also perform a simulated 0–60 mph performance test in both CD and CS modes.[9]

Because the optimal CV and HEV designs are independent of the distance driven per day, we focus on PHEV design and take the HEV and CV to have fixed designs. The HEV design is identical to the Prius model, which has a 57 kW engine, a 52 kW motor, a 168 cell (1.3 kW h) NiMH battery pack, 60.1 mpg efficiency, and 11.0 s 0–60 mpg acceleration time. The CV has a 126 kW engine, 29.5 mpg fuel efficiency, and 11.0 s acceleration time. For the PHEVs, the design variables $\mathbf{x}$ consist of the engine scaling factor x_1, motor scaling factor x_2, battery pack scaling factor x_3, and battery energy swing x_4. To reduce computational time and support global optimization, we created a set of polynomial metamodel fits as functions of $\mathbf{x}$ for the PHEV using discrete simulation data points [22]:[10] (1) CD-mode electricity efficiency η_E (miles/kW h), (2) CS-mode fuel efficiency η_G (mpg), (3) CD-mode 0–60 mph acceleration time t_{CD} (second), (4) CS-mode 0–60 mph acceleration time t_{CS} (second), (5) CD-mode battery energy processed (charging and discharging) per mile μ_{CD} (kW h/mile), (6) CS-mode battery energy processed per mile μ_{CS} (kW h/mile), and (7) final SOC after multiple US06 aggressive driving cycles in CS mode u_{CS} (starting at the target SOC). Metamodels of η_E and η_G are used to calculate energy consumption; t_{CD} and t_{CS} are used to ensure comparison of equivalent-performance vehicles; μ_{CD} and μ_{CS} are used to calculate battery degradation, and u_{CS} is used to ensure that the engine is capable of providing average power needs in CS mode. We evaluated these output values using PSAT over a grid of values for the inputs $x_1 = \{30,45,60\}/57$, $x_2 = \{50,70,90,110\}/52$, and $x_3 = \{200,400,600,800,1000\}/1000$, and multivariate polynomial functions were fit to the data using least squares. The general form of the cubic fitting function f_m is defined as $f_m(\mathbf{x}) = a_{m1}x_1^3 + a_{m2}x_2^3 + a_{m3}x_3^3 + a_{m4}x_1^2x_2 + a_{m5}x_1x_2^2 + a_{m6}x_1^2x_3 + a_{m7}x_1x_3^2 + a_{m8}x_2^2x_3 + a_{m9}x_2x_3^2 + a_{m10}x_1x_2x_3 + a_{m11}x_1^2 + a_{m12}x_2^2 + a_{m13}x_3^2 + a_{m14}x_1x_2 + a_{m15}x_1x_3 + a_{m16}x_2x_3 + a_{m17}x_1 + a_{m18}x_2 + a_{m19}x_3 + a_{m20}$, where the a_m terms are the coefficients for function m. The polynomial fitting coefficients for η_E, η_G, t_{CD}, t_{CS}, μ_{CD}, μ_{CS}, and u_{CS} are listed in Table 3 in the Appendix.[11] The maximum metamodel error among the test points

[6] We exclude public transportation data and vehicles that traveled zero or more than 200 miles. We fit the distribution to the weighted data of total distance traveled on the survey day.

[7] The deviation between data and the exponential fit in the 0–4 mile region has little effect on base case results because 0–4 mile trips contribute little to the social objectives in this study (the curves in Figs. 5(*d*)–5(*f*)).

[8] Examination of alternative driving cycles and the correlation between driving cycle and driving distance is left for future work.

[9] Simulation results are generally optimistic for all vehicles in that they do not account for factors such as vehicle wear, improper maintenance and tire pressure, aggressive driving cycles, extreme accessory loadings, or terrain and weather variation.

[10] An alternative approach for design optimization with metamodel is the Kriging method [23,24], which is not in the scope of this study.

[11] We truncated acceleration data points greater than 13.0 s to improve the metamodel fit and fit μ_{CD}, μ_{CS}, and u_{CS} using quadratic terms to avoid overfitting.

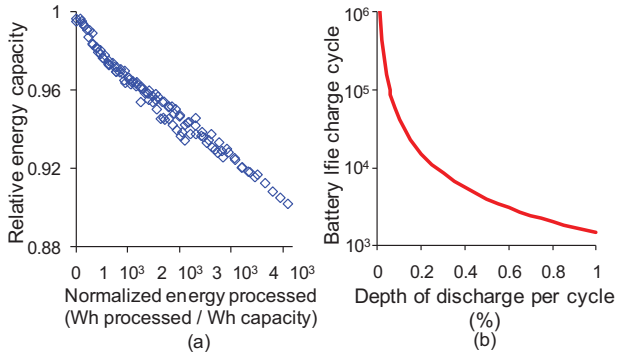

Fig. 4 (*a*) Peterson energy-based degradation model; (*b*) Rosenkranz DOD-based degradation model

is 0.1 miles/kW h, 0.1 mpg, 0.5 s, 0.02 kW h, and 0.5% for electrical efficiency, gasoline efficiency, acceleration time, energy processed, and final SOC, respectively.

2.3 Electric Travel and Battery Degradation. To calculate each objective function, we first define the distance driven on electric power s_E and the distance driven on gasoline s_G as a function of the vehicle's AER s_{AER} and the total distance driven per day s. Assuming one charge per day, s_E and s_G are given by

$$s_E(\mathbf{x},s)=\begin{cases} s & \text{if } s\le s_{AER} \\ s_{AER}(\mathbf{x}) & \text{if } s>s_{AER}\end{cases}$$

$$s_G(\mathbf{x},s)=\begin{cases} 0 & \text{if } s\le s_{AER} \\ s-s_{AER}(\mathbf{x}) & \text{if } s>s_{AER}\end{cases} \tag{4}$$

For PHEVs, we assume that the battery is charged to max SOC once per day. For HEVs and CVs, there is no electric travel; thus, HEV and CV can be seen as special cases with $s_{AER}=0$, so that $s_E=0$ and $s_G=s$. Assuming constant efficiency η_E (miles/kW h) in CD mode, the AER of a PHEV can be calculated from the energy capacity per battery cell $\kappa=0.0216$ kW h/cell, the (scaled) number of cells x_3, and the battery energy swing x_4:

$$s_{AER}(\mathbf{x})=\kappa(1000x_3)x_4\eta_E \tag{5}$$

We consider two distinct battery degradation models from the literature and examine their implications for PHEV design. The Rosenkranz model [13], which has been used in prior PHEV studies [11–14], is based on constant C-rate laboratory discharge tests and views battery degradation as a function of DOD per charge cycle, as shown in Fig. 4(*b*), which cannot predict degradation due to energy use in CS mode. In contrast, the Peterson model [15] was constructed by cycling modern A123 $LiFePO_4$ cells under representative driving cycles (variable C-rate) and measuring capacity fade[12] as a function of energy processed, including intermediate charging and discharging over the driving cycle. Results show relative energy capacity fade as a linear function of normalized energy processed while driving and while charging, as shown in Fig. 4(*a*).

Peterson model. The daily energy processed while driving w_{DRV} and charging w_{CHG} a PHEV can be expressed as

$$w_{DRV}(\mathbf{x},s)=\mu_{CD}s_E+\mu_{CS}s_G,\quad w_{CHG}(\mathbf{x},s)=\frac{s_E}{\eta_E\eta_B} \tag{6}$$

where μ_{CD} and μ_{CS} are energies processed per mile (kW h/mile) in CD and CS modes, respectively, and η_B is battery charging efficiency of 95%. We assume that energy processed for daily charging is equal to net energy consumed in electrical travel per day. The relative energy capacity decrease can be calculated by the energy processed in driving and charging per cycle per cell per original cell energy capacity:

$$r_P(\mathbf{x},s)=\frac{\alpha_{DRV}w_{DRV}+\alpha_{CHG}w_{CHG}}{(1000x_3)\kappa} \tag{7}$$

where $\alpha_{DRV}=3.46\times10^{-5}$ and $\alpha_{CHG}=1.72\times10^{-5}$ are the coefficients for relative energy capacity fade derived from the data set described in Ref. [15].[13] The end of life (EOL) of a battery is defined as the point when the portion of remaining energy capacity is equal to energy swing for the original capacity;[14] the relative energy capacity fade r_{EOL} at the EOL becomes original total capacity minus swing ($r_{EOL}=1-x_4$). The battery life θ_{BAT}, measured in days (or, equivalently, cycles), can be calculated by

$$\theta_{BAT}(\mathbf{x},s)=\frac{r_{EOL}}{r_P}=\frac{1000x_3\kappa(1-x_4)}{\alpha_{DRV}(\mu_{CD}s_E+\mu_{CS}s_G)+\alpha_{CHG}s_E(\eta_E\eta_B)^{-1}} \tag{8}$$

Rosenkranz model. Because we assume that energy consumption is constant in CD mode, energy consumption is proportional to the electric travel distance. If we define maximum SOC at 100%, the energy-based DOD δ is equal to the ratio of the electric travel distance s_E to the maximum distance that could be traveled on the battery's rated capacity:

$$\delta(\mathbf{x},s)=x_4\frac{s_E}{s_{AER}}=\frac{s_E}{\eta_E(1000x_3\kappa)} \tag{9}$$

The battery life θ_{BAT} is estimated using the degradation curve in Fig. 4(*b*):

$$\theta_{BAT}(\mathbf{x},s)=1441\,\delta^{-1.46}=1441\left(\frac{s_E}{\eta_E(1000x_3\kappa)}\right)^{-1.46} \tag{10}$$

2.4 Objective Functions. The objective function in Eq. (2) involves integrals of $f_O(\mathbf{x},s)\cdot f_S(s)$, with $f_S(s)$ defined in Eq. (3) and $f_O(\mathbf{x},s)$ defined below for each objective: minimum petroleum consumption, GHG emissions, and cost. In the petroleum, GHG, and cost cases without discounting, the integral can be written in closed form [26]. The discounted cost cases are solved using numerical integration.

Petroleum consumption. The average gasoline consumed per day $f_G(\mathbf{x},s)$ is given by

$$f_G(\mathbf{x},s)=\frac{s_G(\mathbf{x},s)}{\eta_G(\mathbf{x})} \tag{11}$$

For the HEV and CV cases, Eq. (11) reduces to s/η_G.[15]

Life cycle greenhouse gas emissions. The operating (use phase) GHG emissions v_{OP} represent the average GHG emissions in kg CO_2 equivalent (kg-CO_2-eq) per day associated with the life cycle of gasoline and electricity used to propel the vehicle:

$$v_{OP}(\mathbf{x},s)=\frac{s_E(\mathbf{x},s)}{\eta_E(\mathbf{x})}\frac{v_E}{\eta_C}+\frac{s_G(\mathbf{x},s)}{\eta_G(\mathbf{x})}v_G \tag{12}$$

[12]Deep discharging cycles may cause power fade in Li-ion battery cell [16], which we ignore in this study.

[13]The regression in Ref. [15] focused on finding the degradation from energy arbitrage, but in this paper the regression variables were chosen to enable predictions about degradation due to driving and recharging. The degradation model is optimistic in that it does not account for temperature and time-based degradation; however, future battery designs will likely have improved degradation characteristics.

[14]The industry standard of defining battery EOL as 80% of initial capacity has less optimistic cost implications for PHEVs. We examine this in sensitivity analysis. See also Ref. [25].

[15]Petroleum makes up less than 1.6% of the U.S. electricity grid mix [27], and we ignore it here.

where $\eta_C=88\%$ for battery charging efficiency [28], $v_E=0.752$ kg-CO_2-eq/kW h for electricity emissions,[16] and $v_G=11.34$ kg-CO_2-eq/gal for gasoline life cycle emissions [31]. Total life cycle GHG emissions further include GHGs associated with production of the vehicle and battery. The average total life cycle GHG emissions per day $f_V(\mathbf{x},s)$ is

$$f_V(\mathbf{x},s)=v_{OP}(\mathbf{x},s)+\frac{v_{VEH}}{\theta_{VEH}(s)}+\frac{v_{BAT}}{\theta_{BRPL}(\mathbf{x},s)} \tag{13}$$

where $\theta_{VEH}=s_{LIFE}/s$ is the vehicle life in days, $s_{LIFE}=150,000$ miles [17] is the vehicle life in miles, θ_{BRPL} is the battery replacement effective life (defined below), $v_{BAT}=1000x_3\kappa v_B$ is the battery pack manufacturing emissions, $v_B=120$ kg-CO_2-eq/kW h for Li-ion battery and 230 kg-CO_2-eq/kW h for the NiMH battery is the life cycle GHG emission associated with battery production, $v_{VEH}=8500$ kg-CO_2-eq per vehicle is the life cycle GHG emission associated with vehicle production (excluding emissions from battery production) [2].

Battery replacement scenarios. We consider two battery replacement scenarios. The first is *battery leasing*, $\theta_{BRPL}=\theta_{BAT}$. Each vehicle pays only for the portion of battery life used. The second scenario is *buy lease*, $\theta_{BRPL}=\min(\theta_{BAT},\theta_{VEH})$. If the battery outlasts the life of the vehicle, a single battery pack must be purchased. Partial payment for batteries is not allowed, and new vehicles require new batteries, but if the vehicle outlasts the battery, battery replacement is managed by lease.

Equivalent annualized cost (EAC). To calculate EAC, we define a nominal discount rate r_N, an inflation rate r_I, and the real discount rate $r_R=(1+r_N)/(1+r_I)-1$ [33]. The net present value P of vehicle ownership is the sum of the cost of vehicle operation, vehicle production, and battery costs over the vehicle life:

$$P=\sum_{n=1}^{T}\frac{c_{OP}D(1+r_I)^n}{(1+r_N)^n}+c_{VEH}+\begin{cases}\text{Buy:} & c_{BAT}\\ \text{Lease:} & \displaystyle\sum_{n=1}^{T}\frac{c_{BAT}f_{A|P}(r_N,B)}{(1+r_N)^n}\end{cases} \tag{14}$$

where D is the driving days per year ($D=300$ days in this study), T is the vehicle life in years, and c_{OP} is the sum of the cost of electricity needed to charge the battery and the cost of gasoline consumed,

$$c_{OP}(\mathbf{x},s)=\frac{s_E(\mathbf{x},s)}{\eta_E(\mathbf{x})}\frac{c_E}{\eta_C}+\frac{s_G(\mathbf{x},s)}{\eta_G(\mathbf{x})}c_G \tag{15}$$

$f_{A|P}$ is capital recovery factor for a general discount rate r and time period N in years [33],

$$f_{A|P}(r,N)=\left(\sum_{n=1}^{N}\frac{1}{(1+r)^n}\right)^{-1}=\frac{r(1+r)^N}{(1+r)^N-1} \tag{16}$$

and the net present value of battery leasing cost is calculated by calculating the EAC of the battery over its life B using $f_{A|P}(r_N,B)$ and then summing the present value of annual battery cost over the vehicle life T. The EAC of vehicle ownership is $P\cdot f_{A|P}(r_N,T(s))$, and we divide by D to obtain f_C, the EAC per driving day:

$$f_C(\mathbf{x},s)=c_{OP}\frac{f_{A|P}(r_N,T(s))}{f_{A|P}(r_R,T(s))}+c_{VEH}f_{A|P}(r_N,T(s))D^{-1}+\begin{cases}\text{Buy:} & c_{BAT}f_{A|P}(r_N,T(s))D^{-1}\\ \text{Lease:} & c_{BAT}f_{A|P}(r_N,B(\mathbf{x},s))D^{-1}\end{cases} \tag{17}$$

The vehicle cost (excluding battery pack) c_{VEH} is the sum of vehicle base cost $c_{BASE}=\$11,183$, engine cost $c_{ENG}(x_1)=17.8\times(57x_1)+650$, and motor cost $c_{MTR}(x_2)=26.6\times(52x_2)+520$ [34].[18] The battery pack cost $c_{BAT}=1000x_3\kappa c_B$, where Li-ion battery unit cost $c_B=\$400/\text{kW h}$ (for PHEV only), and the NiMH battery unit cost=$\$600/\text{kW h}$ (for HEV only) in our base case [38].[19] We use the 2008 annual average residential electricity price $c_E=\$0.11/\text{kW h}$ [40] and the 2008 annual average gasoline price $c_G=\$3.30/\text{gal}$ [41] in our base case. For HEV and CV, $s_E=0$, and operating cost consists only of gasoline cost. We relax T and B, allowing noninteger values, with $T(s)=\theta_{VEH}/D=s_{LIFE}/(sD)$ and $B(\mathbf{x},s)=\theta_{BAT}(\mathbf{x},s)/D$. We ignore the possibility of vehicle to grid energy arbitrage for PHEVs since net earning potential is estimated to be low [42], especially under a mass adoption scenario.

2.5 Constraint Functions. To ensure a fair comparison, we require that all vehicles meet an acceleration constraint of 0–60 mph in less than 11 s. Because we have limited our scope to all-electric PHEVs, we require the acceleration constraint to be satisfied both in CD mode, using electric power alone, and in CS mode, where the gasoline engine is also used. The resulting constraints are $t_{CD}(\mathbf{x})\le 11$ s and $t_{CS}(\mathbf{x})\le 11$ s. Additionally, we require the gasoline engine to be large enough to provide average power for the vehicle in CS mode under an aggressive US06 driving cycle while maintaining the target SOC level in the battery. The resulting constraint is $u_{CS}(\mathbf{x})\ge 32\%$. Finally, we impose simple bounds on the decision variables: $30/57\le x_1\le 60/57$, $50/52\le x_2\le 110/52$, $200/1000\le x_3\le 1000/1000$, and $0\le x_4\le 0.8$ to avoid metamodel extrapolation. Any active simple bounds would imply a modeling limitation rather than a physical optimum. As we will later show, of the simple bounds only the upper bounds on battery size and swing are ever active. The upper bound on battery size is reached only when minimizing petroleum consumption since more battery is always preferred for this objective. The upper bound on swing is taken as a practical constraint since (1) SOC cannot be measured precisely, so the battery must be held safely away from the physical capacity, where explosion can occur, and (2) battery resistance, which is relatively flat over most of the SOC window, rises considerably near 0% SOC, causing a drop in efficiency and power output and an increase in heat generation.

3 Results and Discussion

We use the Peterson battery degradation model (Eq. (7)), the buy-lease battery replacement scenario ($\theta_{BRPL}=\min(\theta_{BAT},\theta_{VEH})$), and a 5% nominal discount rate with a 3% inflation rate (the average inflation during 2003–2008 [43]) as our base case. To avoid local minima and numerical issues, we reformulate the problem into a factorable algebraic nonconvex mixed-integer nonlinear program (MINLP) that can be solved globally using the GAMS/BARON convexification-based branch-and-reduce algorithm

[16]The life cycle GHG emissions of electricity is estimated based on the average emissions 0.69 kg-CO_2-eq/kW h of the U.S. grid mixture [29] with 9% transmission loss [30]. We examine alternative grid source scenarios in sensitivity analysis for bounding. For a more detailed dynamic forecast of expected future marginal grid mix associated with PHEV charging, see Ref. [28].

[17]We assume that all vehicles must be replaced every 150,000 miles, the U.S. average vehicle life [32]. This assumption may be unrealistic for vehicles driven very short or very long daily distances because other time-based factors also play a role in vehicle deterioration. We examine implications in sensitivity analysis.

[18]To obtain a comparable vehicle base cost c_{BASE} for PHEV, HEV, and CV, we use the 2008 Prius manufacturer suggested retail price (MSRP) $21,600 and subtract 20% dealer mark-up [35], $3250 NiMH battery pack [36], $1556 base engine cost, and $1902 base motor cost, in 2008 dollars [14,37], ignoring salvage value (future discounting can make battery salvage value insignificant). The resulting vehicle base cost is $c_{BASE}=\$11,183$. We examine alternative cost models in sensitivity analysis.

[19]Future battery costs are uncertain. The Li-ion battery cost of $400/kW h [38], and the NiMH battery cost of $600/kW h [39] are chosen to represent an optimistic but realistic estimate of near-term battery costs in mass production, and we examine a range of costs in our sensitivity analysis.

Table 1 Two-segment results for minimum petroleum, GHG emissions, and cost objectives

Objective			Min Petroleum	Min GHGs		Min Cost	
Optimal vehicle set	CV	HEV	PHEV	PHEV	PHEV	PHEV	HEV
Allocation (miles/day)	0–200	0–200	0–200	0–31	31–200	0–50	50–200
AER (miles)	–	–	87	25	40	20	–
Engine power (kW)	126	57	47	44	47	42	57
Motor power (kW)	–	52	81	71	71	74	52
Number of battery cells	–	168	1000[a]	325	442	251	168
Battery design swing	–	–	0.8[a]	0.68	0.8[a]	0.68	–
Battery capacity (kW h)	–	1.3	21.6	7.0	9.6	5.4	1.3
CD efficiency (miles/kW h)	–	–	5.05	5.33	5.28	5.35	–
CS efficiency (mpg)	29.5	60.1	58.1	60.5	59.9	60.7	60.1
CD 0–60 mph time (s)	–	–	11.0	11.0	11.0	11.0	–
CS 0–60 mph time (s)	11.0	11.0	9.0	9.7	9.1	10.5	11.0
SOC after US06 cycles	–	–	0.32	0.32	0.32	0.32	–
Gasoline (gal/vehicle per day)	1.15	0.57	0.04[b]	0.16		0.38	
GHGs (kg-CO_2-eq/vehicle per day)	15.0	8.41	8.12	7.75[b]		7.92	
Eq. cost ($/vehicle per day)	9.21	7.39	9.05	7.48		7.25[b]	
Reduction versus CV only	–	–	−96%	−48%		−21%	

[a]Variable limited by model boundary.
[b]Optimal objective function value.

[44].[20] Deterministic global optimization, when applicable, avoids the uncertainty and frequently suboptimal solutions of stochastic approaches and offers provable convergence to global minima to facilitate a fair comparison across sensitivity cases [45,46].

3.1 Optimal Solutions. The optimal vehicle type, design, and allocation ranges for two-vehicle segments in each case are summarized in Table 1. The CV and HEV characteristics are included in the first two columns of Table 1 for comparison. To further examine the optimal solutions, we plot the following function values at the optimal solution as a function of driving distance per day in Fig. 5: (1) life cycle equivalent cost, GHG emissions, and gasoline consumption per mile $f_O(\mathbf{x}^*,s)/s$; and (2) the population-weighted equivalent cost, GHG emissions and gasoline consumption per day $f_O(\mathbf{x}^*,s)\cdot f_S(s)$. The area under the population-weighted curve is the objective function. In each case, we compare the CV and HEV performance with the optimal solution.

The optimal solution for minimum petroleum consumption reduces to a single PHEV87 design with the maximum allowed battery size allocated to all drivers.[21] Such a solution is expected since a high-capacity PHEV can travel long distances without using gasoline. Figure 5(*a*) shows the petroleum consumption per mile with respect to the daily driving distance. No gasoline is consumed for driving distances under the AER of 87 miles. Figure 5(*d*) illustrates that moving all drivers from the CV to a PHEV87 reduces net petroleum consumption per vehicle per day (the area under the curve) by 96%.

The optimal two-vehicle solution for minimum GHG emissions is to allocate a medium-range PHEV25 to vehicles that are charged every 31 miles or less (60% of vehicles and 24% of vehicle miles traveled (VMT)) and to allocate a longer-range PHEV40 to vehicles charged less frequently. Assigning all drivers long-range PHEVs can significantly reduce petroleum consumption, but medium-range PHEVs reduce the number of underutilized batteries in these vehicles, reducing the emissions associated with battery production as well as reduced vehicle efficiency caused by carrying heavy batteries.[22] While most vehicles travel short distances (<25 miles) each day (Fig. 3), a greater share of GHG emissions are produced by those vehicles that travel ~25–50 miles/day (Fig. 5(*e*)). A substantial reduction in GHG emissions is achieved by allocating PHEVs or HEVs to drivers rather than CVs, and a modest additional gain is possible by segmenting the population and allocating the right PHEV to the right driver.

The minimum cost solution in the base case is to assign PHEV20s to vehicles that drive 50 miles or less each day (77% of vehicles and 43% of VMT) and assign ordinary HEVs to vehicles charged less frequently. Figure 5(*c*) shows that equivalent cost per mile is high for drivers who travel short daily distances because short daily distances imply long vehicle life, capital costs dominate operation costs for these vehicles, and annualized capital costs are divided over small distances.[23] When population weighting is included, Fig. 5(*f*) reveals a small but noticeable PHEV benefit for drivers who travel ~5–40 miles/day.

An important observation is that the optimal battery designs have generally high swing values, ranging from 68% to the upper bound 80%. The degradation mechanism based on energy processed implies that designers can allow more of the battery to be used, even though this will require battery replacement for some drivers.

3.2 Sensitivity Analyses. We conduct sensitivity analyses using three vehicle segments to examine the minimum cost and GHG solutions for alternative scenarios and characterize the robustness of our conclusions. The major cost scenarios include (1) Li-ion battery cost of $250–1000/kW h [47,48], (2) gasoline price of $1.50–6.00/gal [41], (3) electricity price of $0.06–0.30/kW h [49], (4) discount rate of 0–10%, and (5) carbon allowance price of $0–100/metric ton of CO_2 equivalent (ton-CO_2-eq) [42]. The optimal vehicles and allocation for these sensitivity analyses are

[20]The detailed MINLP reformulation is available in Ref. [26] or by contacting the authors. In the discounted cost cases, the integral in the objective function does not reduce to a closed form expression, so we use numerical integration with random multistart approach. Comparisons with known global solutions in Ref. [26] suggest high confidence of global optimality for the multistart solutions.

[21]We use the notation PHEV*x* to denote a PHEV with an AER of *x* miles.

[22]For a daily travel distance of 30 miles, about 85% of CV emissions and 75% of electrified vehicle emissions are associated with the use phase, while battery production emissions contribute less than 5% of life cycle GHGs for a PHEV40. These ratios are similar to the findings in Ref. [2].

[23]When driven 30 miles/day, vehicle capital cost is about half of annualized cost of CV ownership, whereas it makes up 90% if driven only 1 mile/day. By comparison, at 30 miles/day vehicle capital cost is about 70% of annualized cost for HEVs and 80% of annualized cost for a PHEV20, with 10% of capital costs due to batteries.

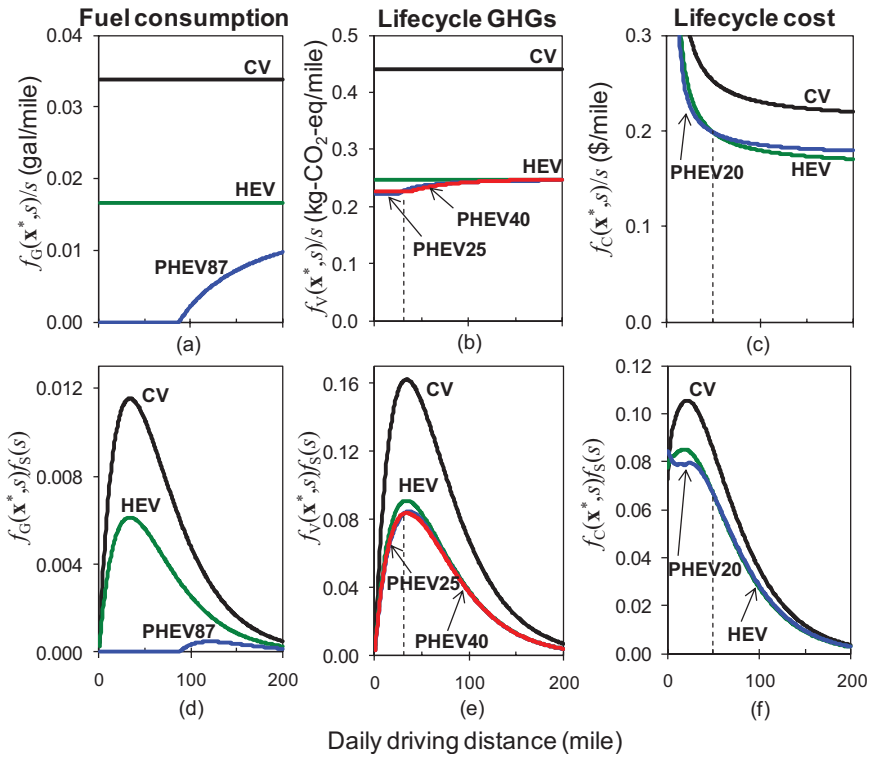

Fig. 5 Optimal two-segment PHEV design and allocations for minimizing petroleum consumption, life cycle cost, and GHG emissions for the base case scenario

summarized in Fig. 6. The horizontal axis shows the portion of vehicles, daily travel distance, and portion of VMT allocated to each vehicle, and the allocation distance cutoff point is labeled where appropriate. Our three-segment[24] minimum cost base case solution allocates a PHEV16 (4.9 kW h battery pack at 59% swing) to vehicles that travel 20 miles/day or less, a PHEV25 (6.7 kW h battery pack at 71% swing) to vehicles traveling 20–51 miles/day, and a HEV to the remaining drivers, resulting in an equivalent net life cycle cost of $7.23 per vehicle/day. While less than 25% of vehicles are HEVs in this scenario, they represent more than half of VMT because HEVs are allocated to high-mileage vehicles.

High battery costs, low gas prices, and high electricity prices are not beneficial to PHEVs, and the HEV is the lowest cost alternative in these cases. Low electricity prices make higher-capacity PHEVs more competitive for more drivers. Low electricity prices are associated with off-peak charging; however, off-peak rates would likely increase under high PHEV penetration scenarios. Similarly, low Li-ion battery costs or high gasoline prices improve the economic performance of PHEVs and make them cost competitive for a wide range of drivers. Variation in HEV NiMH battery cost from $440 to $700/kW h [39] (not shown) has a marginal effect, moving the optimal HEV allocation cutoff from 45 to 55 miles/day, respectively.

Higher discount rates make PHEVs less competitive due to higher upfront purchase cost with operation cost savings in the future. With $400/kW h Li-ion costs, PHEVs are part of the least-cost solution at nominal discount rates below 11%. A 0% discount rate results in a slightly increased PHEV allocation up to 55 miles/day. At a 5% discount rate, PHEVs are part of the least-cost solution for battery pack prices below $590/kW h, and at 10% pack prices must be below $410/kW h.

Carbon allowance prices applied to all carbon emissions in the supply chain assuming 100% pass-through produce only marginal

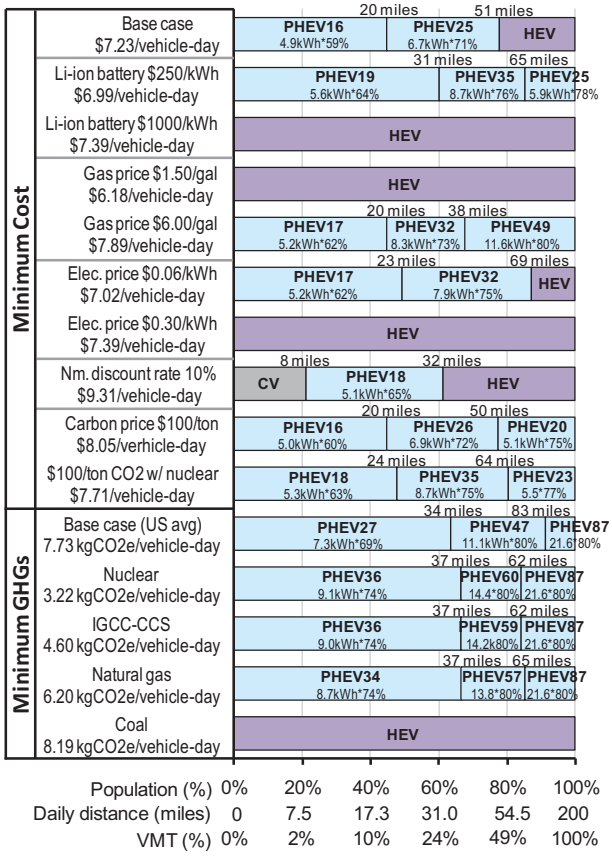

Fig. 6 Optimal three-segment vehicle design and allocation for various scenarios. The base case assumes the buy-lease battery scenario, Peterson battery degradation model, $400/kW h Li-ion cost, $600/kW h NiMH cost, $3.30/gal gasoline, $0.11/kW h electricity, average U.S. grid GHG emissions, $0/ton-$CO_2$-eq allowance price, and 5% discount rate.

[24]The minimum cost in the three-vehicle case is 0.3% lower than the two-vehicle case, indicating that further vehicle segmentation refinement is of marginal value.

changes in life cycle cost competitiveness of PHEVs. CO_2 prices as high as \$100/ton-CO_2-eq make PHEVs cost competitive with HEVs only if vehicle costs are already comparable.[25] For our base case, a cost of \$83/ton-CO_2-eq is required to replace HEV allocation with PHEVs; however, the critical CO_2 price for affecting allocation varies widely under alternative assumptions of discount rate and energy and battery prices. Under a low carbon nuclear electricity scenario, a \$100/ton CO_2 price encourages slightly larger battery packs.

We examined alternative assumptions for vehicle costs, with vehicle base costs of \$9000-13,000 and alternative engine/motor cost models from Ref. [48], but solutions are robust. Tax incentives for PHEV batteries from the American Recovery and Reinvestment Act (ARRA) [52] incentivize allocation of more PHEVs with larger battery packs; however, including taxpayer cost of the incentives and \$100/ton CO_2 externality costs, the optimal solution under American Recovery and Reinvestment Act (ARRA) incentives results in 6% higher net costs than under a \$100/ton CO_2 tax scenario. We also examined several alternative battery assumptions: First, a policy scenario where battery life is required to outlast vehicle life shows little change in the PHEV designs with optimized swings reduced 2–5% compared with the base case solution. The battery leasing scenario, which allows prorated payment for partial battery use, results in larger packs with reduced swing and improved PHEV competitiveness. Defining battery EOL at 20% capacity fade [15] makes PHEVs less competitive and incentivizes maximum swing [25]. The Rosenkranz DOD-based degradation model, which encourages shallow swing to preserve battery life, results in a PHEV11 (5.2 kW h at 39% swing—a battery size equivalent to a PHEV23 at 80% swing) for 2–26 miles/day and a HEV for higher-mileage vehicles. Thus, the best used strategy for PHEV battery swing depends on the degradation mechanism. Planned PHEVs such as the Chevrolet Volt report a swing of around 50% in order to maintain battery life [53]. The Rosenkranz model is based on older battery technology, constant rate charge and discharge cycles, and no accounting for degradation in CS mode, while the Peterson model, which tests $LiFePO_4$ cells with representative cycling [15], suggests that designers should use smaller battery packs with a larger swing.

We examine the optimal solution for minimizing life cycle GHG emissions with different grid emission scenarios, which include (1) nuclear (0.066 kg-CO_2-eq/kW h) [54], (2) integrated gasification combined cycle with carbon capture and sequestration (IGCC-CCS) (0.252 kg-CO_2-eq/kW h) [55], (3) natural gas (0.47 kg-CO_2-eq/kW h) [56], and (4) coal (0.9 kg-CO_2-eq/kW h) [56].[26] These cases are intended to encompass the range of potential regional and marginal dispatch grid mix scenarios. Figure 6 shows that minimum GHG solutions involve higher-capacity PHEVs under low carbon grid scenarios and no PHEVs in the coal scenario. Life cycle emissions are 150% higher under optimal coal versus optimal nuclear scenarios, and natural gas, which is often used for marginal dispatch, has lower emissions than the U.S. average. Carbon content in electricity generation can significantly affect the GHG implications of PHEVs [2,57,58].

4 Conclusions

We construct an optimization model to determine the optimal vehicle design and allocation of conventional, hybrid, and plug-in hybrid vehicles to drivers in order to minimize life cycle cost, petroleum consumption, and GHG emissions. In our base case, we find that (1) minimum petroleum consumption is achieved by assigning high-range PHEVs to all drivers; (2) minimum life cycle GHG emissions are achieved by assigning a mix of low-range (~25 miles) PHEVs and midrange (40–50 miles) PHEVs; and (3) minimum life cycle cost is achieved by assigning low-range (15–25 miles) PHEVs to the ~75% of drivers who travel less than ~50 miles/day and HEVs to drivers who travel further. Optimal allocation of vehicles to drivers appears to be of second-order importance for net life cycle cost and GHG emissions compared with an overall shift from CVs to HEVs or PHEVs.

Under our base case assumptions, life cycle costs and GHGs of HEVs and PHEVs are comparable, particularly for drivers who charge frequently, and the least-cost solution is sensitive to the discount rate and the price of gasoline, electricity, and batteries. Relative to our base case of \$3.30/gal gasoline, \$0.11/kW h electricity, \$400/kW h Li-ion batteries, \$600/kW h NiMH batteries, and 5% discount rate, PHEVs are part of the least-cost solution for gas prices above \$2.6/gal, electricity prices below \$0.16/kW h, Li-ion battery prices below \$590/kW h, or nominal discount rates below 11%. At a 10% discount rate, Li-ion pack cost must fall below \$410/kW h for PHEVs to be part of the least-cost solution. Consumers are often observed to use discount rates above 10% in practice [59–61], so battery pack costs significantly below \$400/kW h may be needed to drive mass consumer adoption unless gasoline prices rise.

Carbon allowance prices applied to all life cycle CO_2 emissions with 100% pass-through have marginal impact on PHEV economic competitiveness, as noted by Kammen et al. [62] and by Plotkin and Singh [48]. For example, when driven 20 miles/day using the U.S. average grid mix, a HEV has net life cycle emissions of about 0.1 kg CO_2-eq/vehicle per day greater than the PHEV20. A \$100/ton allowance price translates to a \$0.11/vehicle per day greater penalty for the HEV than for the PHEV20. This is not enough to make PHEVs more economical than HEVs unless life cycle costs of PHEVs are already within about \$350 (~1.5%) of HEV life cycle costs. As an upper bound, a highly optimistic scenario of low carbon electricity (nuclear) at base electricity prices (\$0.11/kW h) and \$100/ton allowance prices produces ~\$0.59/day greater penalty for HEVs than PHEVs. This is not enough to make PHEVs more economical than HEVs unless PHEV life cycle costs already fall within about \$1900 (~8%) of HEV costs (or within \$1500, ~7%, at a 10% discount rate). Under most scenarios, CO_2 prices offer little leverage for improving cost competitiveness of PHEVs, and PHEV life cycle costs must fall within a few percent of HEV costs in order to offer a cost-effective approach to GHG reduction.[27]

Using recent $LiFePO_4$ degradation models based on energy processed in place of prior DOD-based degradation models, we find that life cycle cost, GHG emissions, and petroleum consumption are minimized using higher battery swing (above 60%) and replacing batteries as needed, rather than designing underutilized capacity into the vehicle with corresponding production, weight, and cost implications. This contrasts with the current practice of restricting swing to values near 50% to improve battery life. Allowing optimized swing rather than restricting swing to 50% reduces life cycle cost and GHGs of PHEVs by about 1–2% in our model—small enough that other factors such as logistics, customer satisfaction, regulation, and incentives may play a significant role in determining battery swing in PHEV design. Current incentives for PHEVs, such as those outlined in the ARRA [52], provide subsidies based on battery size, rather than usable battery capacity, all-electric range, or effective GHG reduction. This encourages more PHEVs with larger battery packs but results in increased social costs[28] and could produce unintended incentives for battery swing selection. PHEV battery subsidies are likely

[25]The National Research Council estimated environmental damage costs of carbon emissions as \$10–100 per ton-CO_2-eq, with a middle estimate of \$30 [50], and the Department of Energy projects carbon allowance prices of \$20–93/ton from the Waxman–Markey bill by 2020 [51].

[26]The emission factors are at the power plant gate, and 9% transmission and distribution loss to outlet is applied in the PHEV GHG calculations [30].

[27]For comparison, using the most optimistic 2050 emission scenarios in Ref. [28], NPV of CO_2 cost savings for PHEVs over HEVs at \$100/ton and 5% discounting are around \$1100 or about 4.6% of HEV life cycle cost.

[28]We do not account for social costs of petroleum consumption or criteria pollutants here.

only economically justified as a temporary stimulus if battery and energy costs are expected to quickly reach levels that make PHEVs cost competitive with HEVs over the life cycle.

5 Limitations and Future Work

The proposed model contains a number of assumptions that should be understood in order to interpret results meaningfully. These assumptions fall into four major categories: decision scope, driver behavior, technology scope, and endogeneity.

We examine a benevolent dictator's optimal choices of vehicle design and allocation to meet personal transportation needs in the U.S. with minimum equivalent daily cost, GHG emissions, or petroleum consumption. This scenario is useful for understanding the relationship between design/allocation and social objectives; however, the market behavior may deviate. In particular, consumers may value purchase price over future petroleum cost savings with hyperbolic discounting, and they may value correlated vehicle attributes that are not considered here, such as convenience or interior space [63].

Second, we make several assumptions about the driver behavior. While we account for across-driver heterogeneity in daily distance traveled, we lack data on within-driver variation, so our results overestimate the potential of optimal allocation. However, we find optimal allocation to be of second-order importance even in this scenario. We ignore potential changes in driving patterns due to reduced operating cost and changes in vehicle technology. Additionally, we assume that each PHEV driver charges once per day, and we ignore the cost of charging infrastructure. Allowing multiple daily charges would require additional charging infrastructure and would give PHEVs a longer effective AER [64]. Finally, we use the UDDS cycle to estimate vehicle efficiency for all drivers, which may produce optimistic predictions for both range and efficiency in real-world driving, and we ignore regional variation in driving style, terrain, weather, and grid characteristics [57,65–67]. Our base case use of average U.S. grid characteristics to calculate GHG emissions may over- or underestimate emissions associated with particular regions, charge timing, and marginal dispatch [57]; however, our sensitivity analysis bounds the range of possible scenarios [28,57].

The third class of modeling assumptions involves technology scope. We assume a fixed Li-ion battery technology for PHEVs with performance models based on a Saft cell and degradation data from A123 cells. In practice, different battery designs may be used for different vehicle systems [11,68,69], and we leave such assessment for future work. We assume a static battery technology with a base cost of $400/kW h installed pack cost, intended to represent an optimistic but realistic future scenario, particularly for thick-electrode high-energy batteries used for larger packs [11,38]. Dynamics of technology advancement and cost reduction could have strategic implications for vehicle system design and allocation [70]. We examine only energy-processed based degradation mechanisms and ignore temperature effects and calendar (storage) degradation mechanisms that affect batteries when not in use. Future work is needed to characterize these temperature and time-based mechanisms, although they would be expected to further encourage a large swing and to make PHEVs somewhat less competitive. Moreover, future battery technology may have improved degradation characteristics, which can change PHEV design implications. We also limit our study to all-electric PHEVs with characteristics similar to a Toyota Prius. Blended-mode PHEVs that make use of the gasoline engine during CD mode offer additional control flexibility and the ability to design vehicles with smaller motors and battery packs [71]. An analysis of blended-mode PHEVs requires examination of the space of control strategy variables, and we leave this and the study of different vehicle classes for future work.

Finally, we treat energy prices and grid characteristics as exogenous factors. A significant shift to PHEVs may influence the price of gasoline, electricity, or batteries or the mix of electricity generation modes (because of new plant construction or increase in off-peak demand) [28,57]. We leave the examination of these potentially endogenous relationships for future work.

Acknowledgment

The authors would like to thank Paulina Jaramillo, Constantine Samaras, and the members of the Design Decisions Laboratory, the Carnegie Mellon Green Design Institute and xEV Group for their feedback and help with model formulation. This research was supported in part by grants from the National Science Foundation's CAREER program (Award No. 0747911) and the Material Use, Science, Engineering and Society (MUSES) program (Award No. 0628084), the Liang Ji-Dian Fellowship (Shiau), the ICES Dowd Fellowship (Peterson), and grants from Ford Motor Co. and Toyota Motor Corporation.

Appendix

See Tables 2 and 3.

Table 2 Vehicle configurations in simulation

Module	Property	CV	HEV	PHEV
Vehicle body and chassis	F/R weight ratio	0.6/0.4	0.6/0.4	0.6/0.4
	Drag coefficient	0.26	0.26	0.26
	Frontal area (m^2)	2.25	2.25	2.25
	Tire specs	P175/65 R14	P175/65 R14	P175/65 R14
	Body mass (kg)	824	824	824
Engine	Power (kW)	126	57	30–60
	Mass (kg)	296	114	50–110
Motor	Power (kW)	–	52	50–110
	Mass (kg)	–	65	40–143
Battery	No. of cells	–	168	200–1000
	Mass (kg)	–	36	60–419
Electrical accessory	Power (kW)	0.8	0.8	0.8
	Net weight (kg)	1709	1520	1497–1995

Table 3 Polynomial coefficients of the PHEV performance metamodel

f_m	η_E	η_G	t_{CD}	t_{CS}	μ_{CD} [a]	μ_{CS} [a]	u_{CS} [a]
m	1	2	3	4	5	6	7
a_{m1}	0.008	2.214	1.457	3.334			
a_{m2}	0.154	1.087	−5.496	−2.266			
a_{m3}	0.353	5.578	−28.46	−20.26			
a_{m4}	−0.005	−0.815	0.913	0.414			
a_{m5}	−0.005	0.510	−0.881	−3.524			
a_{m6}	−0.025	1.562	−1.050	−0.286			
a_{m7}	0.000	2.212	−0.308	−10.11			
a_{m8}	−0.057	−0.613	2.044	1.951			
a_{m9}	−0.043	0.254	15.61	10.31			
a_{m10}	−0.016	−0.159	0.336	5.808			
a_{m11}	−0.001	−8.906	−4.634	−6.932	0.001	0.063	−0.194
a_{m12}	−0.805	−6.095	31.48	15.80	0.002	−0.001	−0.005
a_{m13}	−0.656	−15.21	34.02	39.20	0.007	−0.002	0.047
a_{m14}	0.057	0.089	1.153	7.901	0.000	−0.002	0.000
a_{m15}	0.080	−3.274	1.169	6.582	0.001	−0.005	0.011
a_{m16}	0.342	2.498	−32.06	−30.12	−0.001	0.001	−0.001
a_{m17}	−0.191	2.622	3.405	−6.734	0.013	−0.120	0.382
a_{m18}	1.189	9.285	−54.47	−26.39	0.005	0.010	0.019
a_{m19}	−0.347	5.837	9.570	−4.098	0.050	0.054	−0.077
a_{m20}	4.960	57.68	44.23	32.10	0.296	0.194	0.140

[a]The terms are fit with quadratic form.

References

[1] Bandivadekar, A., Bodek, K., Cheah, L., Evans, C., Groode, T., Heywood, J., Kasseris, E., Kromer, M., and Weiss, M., 2008, "On the Road in 2035: Reducing Transportation's Petroleum Consumption and GHG Emissions," Massachusetts Institute of Technology, Report No. LFEE 2008-05 RP.

[2] Samaras, C., and Meisterling, K., 2008, "Life Cycle Assessment of Greenhouse Gas Emissions From Plug-in Hybrid Vehicles: Implications for Policy," Environ. Sci. Technol., **42**(9), pp. 3170–3176.

[3] Bureau of Transportation Statistics, 2003, "National Household Travel Survey 2001," U.S. Department of Transportation.

[4] Vlasic, B., and Bunkley, N., 2009, "G.M. Puts Electric Car's City Mileage in Triple Digits," The New York Times, http://www.nytimes.com/2009/08/12/business/12auto.html.

[5] Toyota, 2009, "2010 Prius Plug-in Hybrid Makes North American Debut at Los Angeles Auto Show," http://pressroom.toyota.com/pr/tms/toyota/2010-prius-plug-in-hybrid-makes-149402.aspx, accessed on Jul. 12, 2010.

[6] Frank, A. A., 2007, "Plug-in Hybrid Vehicles for a Sustainable Future," Am. Sci., **95**(2), pp. 158–165.

[7] Zhang, Y., Lin, H., Zhang, B., and Mi, C., 2006, "Performance Modeling and Optimization of a Novel Multi-Mode Hybrid Powertrain," ASME J. Mech. Des., **128**(1), pp. 79–89.

[8] Markel, T., Brooker, A., Gonder, J., O'Keefe, M., Simpson, A., and Thornton, M., 2006, "Plug-in Hybrid Vehicle Analysis," National Renewable Energy Laboratory, Report No. NREL/MP-540-40609.

[9] Shiau, C. S. N., Samaras, C., Hauffe, R., and Michalek, J. J., 2009, "Impact of Battery Weight and Charging Patterns on the Economic and Environmental Benefits of Plug-in Hybrid Vehicles," Energy Policy, **37**(7), pp. 2653–2663.

[10] Hall, J. C., Lin, T., and Brown, G., 2006, "Decay Processes and Life Predictions for Lithium Ion Satellite Cells," Fourth International Energy Conversion Engineering Conference and Exhibit (IECEC), San Diego, CA, Jun. 26–29, Paper No. AIAA 2006-4078.

[11] Kromer, M. A., and Heywood, J. B., 2009, "A Comparative Assessment of Electric Propulsion Systems in the 2030 US Light-Duty Vehicle Fleet," SAE Int. J. Engines, **1**(1), pp. 372–391.

[12] Markel, T., and Simpson, A., 2006, "Plug-in Hybrid Electric Vehicle Energy Storage System Design," Advanced Automotive Battery Conference, Baltimore, MD, May 17–19.

[13] Rosenkranz, K., 2003, "Deep-Cycle Batteries for Plug-in Hybrid Application," EVS20 Plug-In Hybrid Vehicle Workshop, Long Beach, CA.

[14] Simpson, A., 2006, "Cost-Benefit Analysis of Plug-in Hybrid Electric Vehicle Technology," Proceedings of the 22nd International Battery, Hybrid and Fuel Cell Electric Vehicle Symposium and Exhibition (EVS-22), Yokohama, Japan, Oct. 23–28.

[15] Peterson, S. B., Whitacre, J. F., and Apt, J., 2010, "Lithium-Ion Battery Cell Degradation Resulting From Realistic Vehicle and Vehicle-to-Grid Utilization," J. Power Sources, **195**(8), pp. 2385–2392.

[16] Belt, J. R., Ho, C. D., Motloch, C. G., Miller, T. J., and Duong, T. Q., 2003, "A Capacity and Power Fade Study of Li-Ion Cells During Life Cycle Testing," J. Power Sources, **123**(2), pp. 241–246.

[17] Cooper, A. B., Georgiopoulos, P., Kim, H. M., and Papalambros, P. Y., 2006, "Analytical Target Setting: An Enterprise Context in Optimal Product Design," ASME J. Mech. Des., **128**(1), pp. 4–13.

[18] Michalek, J. J., Papalambros, P. Y., and Skerlos, S. J., 2004, "A Study of Fuel Efficiency and Emission Policy Impact on Optimal Vehicle Design Decisions," ASME J. Mech. Des., **126**(6), pp. 1062–1070.

[19] Federal Highway Administration, 2010, "National Household Travel Survey 2009," Department of Transportation, Washington, D.C.

[20] Argonne National Laboratory, 2008, Powertrain Systems Analysis Toolkit (PSAT).

[21] Environmental Protection Agency, 2010, "Dynamometer Drive Schedules," http://www.epa.gov/nvfel/testing/dynamometer.htm, accessed on Jul. 12.

[22] Shan, S., and Wang, G. G., 2010, "Metamodeling for High Dimensional Simulation-Based Design Problems," ASME J. Mech. Des., **132**(5), p. 051009.

[23] Li, M. L. G., and Azarm, S., 2008, "A Kriging Metamodel Assisted Multi-Objective Genetic Algorithm for Design Optimization," ASME J. Mech. Des., **130**(3), p. 031401.

[24] Martin, J. D., 2009, "Computational Improvements to Estimating Kriging Metamodel Parameters," ASME J. Mech. Des., **131**(8), p. 084501.

[25] Shiau, C.-S. N., Peterson, S. B., and Michalek, J. J., 2010, "Optimal Plug-in Hybrid Electric Vehicle Design and Allocation for Minimum Life Cycle Cost, Petroleum Consumption and Greenhouse Gas Emissions," ASME 2010 International Design Engineering Technical Conferences, Montreal, Quebec, Canada, Paper No. DETC2010-28198.

[26] Shiau, C.-S. N., and Michalek, J. J., 2010, "A Mixed-Integer Nonlinear Programming Model for Deterministic Global Optimization of Plug-in Hybrid Vehicle Design and Allocation," ASME 2010 International Design Engineering Technical Conferences, Montreal, Quebec, Canada, Paper No. IDETC2010-28064.

[27] Energy Information Administration, 2009, "Electric Power Annual 2007," U.S. Department of Energy, DOE/EIA-0348(2007), http://www.eia.doe.gov/cneaf/electricity/epa/epa.pdf, accessed on Jul. 12, 2010.

[28] EPRI, 2007, "Environmental Assessment of Plug-in Hybrid Electric Vehicles. Volume 1: Nationwide Greenhouse Gas Emissions," Electric Power Research Institute.

[29] Weber, C. L., Jaramillo, P., Marriott, J., and Samaras, C., 2010, "Life Cycle Assessment and Grid Electricity: What Do We Know and What Can We Know?" Environ. Sci. Technol., **44**(6), pp. 1895–1901.

[30] Energy Information Administration, 2008, "Annual Energy Review 2007," U.S. Department of Energy, http://www.eia.doe.gov/emeu/aer/elect.html, accessed on Jul. 12, 2010.

[31] Wang, M., Wu, Y., and Elgowainy, A., 2007, "GREET 1.7 Fuel-Cycle Model for Transportation Fuels and Vehicle Technologies," Argonne National Laboratory, Argonne, IL.

[32] Environmental Protection Agency, 2006, "Emission Durability Procedures and Component Durability Procedures for New Light-Duty Vehicles, Light-Duty Trucks and Heavy-Duty Vehicles; Final Rule and Proposed Rule," http://www.epa.gov/EPA-AIR/2006/January/Day-17/a074.pdf, accessed on Jul. 12, 2010.

[33] Neufville, R. D., 1990, *Applied Systems Analysis: Engineering Planning and Technology Management*, McGraw-Hill, New York.

[34] EPRI, 2001, "Comparing the Benefits and Impacts of Hybrid Electric Vehicle Options," Electric Power Research Institute, Palo Alto, CA.

[35] Lipman, T. E., and Delucchi, M. A., 2006, "A Retail and Lifecycle Cost Analysis of Hybrid Electric Vehicles," Transp. Res. D, **11**(2), pp. 115–132.

[36] Naughton, K., 2008, "Assaulted Batteries," Newsweek, Jul. 2, 2008, http://www.newsweek.com/id/138808, accessed on Jul. 12, 2010.

[37] Bureau of Labor Statistics, 2009, "Producer Price Indexes," U.S. Department of Labor.

[38] Whitacre, J. F., 2009, "The Economics and Science of Materials for Lithium Ion Batteries and PEM Fuel Cells," Working paper, Carnegie Mellon University, Pittsburgh, PA.

[39] Duvall, M., 2004, "Advanced Batteries for Electric-Drive Vehicles," Electric Power Research Institute, Palo Alto, CA.

[40] Energy Information Administration, 2009, "Average Retail Price of Electricity to Ultimate Customers: Total by End-Use Sector," U.S. Department of Energy, http://www.eia.doe.gov/cneaf/electricity/epm/table5_3.html, accessed on Jul. 12, 2010.

[41] Energy Information Administration, 2009, "The U.S. Weekly Retail Gasoline and Diesel Prices," U.S. Department of Energy, http://tonto.eia.doe.gov/dnav/pet/pet_pri_gnd_dcus_nus_a.htm, accessed on Jul. 12, 2010.

[42] Peterson, S. B., Whitacre, J. F., and Apt, J., 2010, "The Economics of Using Plug-in Hybrid Electric Vehicle Battery Packs for Grid Storage," J. Power Sources, **195**(8), pp. 2377–2384.

[43] U.S. Bureau of Labor Statistics, http://www.bls.gov/data/inflation_calculator.htm, accessed on Jul. 12, 2010.

[44] Tawarmalani, M., and Sahinidis, N. V., 2004, "Global Optimization of Mixed-Integer Nonlinear Programs: A Theoretical and Computational Study," Math. Program., **99**(3), pp. 563–591.

[45] Khajavirad, A., and Michalek, J. J., 2009, "A Deterministic Lagrangian-Based Global Optimization Approach for Quasiseparable Nonconvex Mixed-Integer Nonlinear Programs," ASME J. Mech. Des., **131**(5), p. 051009.

[46] Rao, S. S., and Xiong, Y., 2005, "A Hybrid Genetic Algorithm for Mixed-Discrete Design Optimization," ASME J. Mech. Des., **127**(6), pp. 1100–1112.

[47] Lemoine, D. M., Kammen, D. M., and Farrell, A. E., 2008, "An Innovation and Policy Agenda for Commercially Competitive Plug-in Hybrid Electric Vehicles," Environ. Res. Lett., **3**, p. 014003.

[48] Plotkin, S., and Singh, M., 2009, "Multi-Path Transportation Futures Study: Vehicle Characterization and Scenario Analyses," Argonne National Laboratory, Report No. ANL/ESD/09-5.

[49] Yura, J. K., 2009, "Electric Schedule E-9: Experimental Residential Time-of-Use Service for Low Emission Vehicle Customers," Pacific Gas and Electric Company, San Francisco, CA.

[50] National Research Council, 2009, *Hidden Costs of Energy: Unpriced Consequences of Energy Production and Use*, The National Academies, Washington, D.C.

[51] Energy Information Administration, 2009, "Energy Market and Economic Impacts of H.R. 2454, the American Clean Energy and Security Act of 2009," Department of Energy, http://www.eia.doe.gov/oiaf/servicerpt/hr2454/pdf/sroiaf%282009%2905.pdf, accessed on Jul. 12, 2010.

[52] U.S. Congress, 2008, "American Recovery and Reinvestment Act of 2009," http://fdsys.gpo.gov/fdsys/pkg/BILLS-111hr1ENR/pdf/BILLS-111hr1ENR.pdf, accessed on Jul. 12, 2010.

[53] gm-volt.com, 2009, "Latest Chevy Volt Battery Pack and Generator Details and Clarifications," http://gm-volt.com/2007/08/29/latest-chevy-volt-battery-pack-and-generator-details-and-clarifications/, accessed on Jul. 12, 2010.

[54] Sovacool, B. K., 2008, "Valuing the Greenhouse Gas Emissions From Nuclear Power: A Critical Survey," Energy Policy, **36**(8), pp. 2950–2963.

[55] Jaramillo, P., Samaras, C., Wakeley, H., and Meisterling, K., 2009, "Greenhouse Gas Implications of Using Coal for Transportation: Life Cycle Assessment of Coal-to-Liquids, Plug-in Hybrids, and Hydrogen Pathways," Energy Policy, **37**(7), pp. 2689–2695.

[56] Weisser, D., 2007, "A Guide to Life-Cycle Greenhouse Gas (GHG) Emissions From Electric Supply Technologies," Energy, **32**(9), pp. 1543–1559.

[57] Sioshansi, R., and Denholm, P., 2009, "Emissions Impacts and Benefits of Plug-in Hybrid Electric Vehicles and Vehicle-to-Grid Services," Environ. Sci. Technol., **43**(4), pp. 1199–1204.

[58] Huo, H., Zhang, Q., Wang, M. Q., Streets, D. G., and He, K., 2010, "Environmental Implication of Electric Vehicles in China," Environ. Sci. Technol., **44**(13), pp. 4856–4861.

[59] Dreyfus, M. K., and Viscusi, W. K., 1995, "Rates of Time Preference and Consumer Valuations of Automobile Safety and Fuel Efficiency," J. Law Econom., **38**(1), pp. 79–105.

[60] Hassett, K. A., and Metcalf, G., 1993, "Energy Conservation Investment: Do Consumers Discount the Future Correctly?" Energy Policy, **21**(6), pp. 710–716.
[61] Train, K., 1985, "Discount Rates in Consumers' Energy-Related Decisions," Energy, **10**(12), pp. 1243–1253.
[62] Kammen, D. M., Arons, S. M., Lemoine, D. M., and Hummel, H., 2009, "Cost Effectiveness of Greenhouse Gas Emission Reductions From Plug-in Hybrid Electric Vehicles," *Plug-in Electric Vehicles-What Role for Washington?*, D. B. Sandalow, ed., Brookings Institution, Washington, D.C.
[63] Allcott, H., and Wozny, N., 2009, "Gasoline Prices, Fuel Economy, and the Energy Paradox," Working paper, MIT Department of Economics, Cambridge, MA.
[64] Bradley, T. H., and Frank, A. A., 2009, "Design, Demonstrations and Sustainability Impact Assessments for Plug-in Hybrid Electric Vehicles," Renewable Sustainable Energy Rev., **13**, pp. 115–128.
[65] Gonder, J., Markel, T., Simpson, A., and Thornton, M., 2007, "Using GPS Travel Data to Assess the Real World Driving Energy Use of PHEVs," Transportation Research Board Annual Meeting, Washington, D.C., Jan. 21–25.
[66] Moawad, A., Singh, G., Hagspiel, S., Fellah, M., and Rousseau, A., 2009, "Impact of Real World Drive Cycles on PHEV Fuel Efficiency and Cost for Different Powertrain and Battery Characteristics," The 24th International Electric Vehicle Symposium and Exposition (EVS-24), Stavanger, Norway, May 13–16.
[67] Patil, R., Adornato, B., and Filipi, Z., 2009, "Impact of Naturalistic Driving Patterns on PHEV Performance and System Design," Working paper, University of Michigan, Ann Arbor, MI.
[68] Albertus, P., and Newman, J., 2008, "A Simplified Model for Determining Capacity Usage and Battery Size for Hybrid and Plug-in Hybrid Electric Vehicles," J. Power Sources, **183**(1), pp. 376–380.
[69] Pesaran, A., Markel, T., Tataria, H., and Howell, D., 2007, "Battery Requirements for Plug-in Hybrid Electric Vehicles—Analysis and Rationale," The 23th International Electric Vehicle Symposium (EVS-23), Anaheim, CA, Dec. 2–5.
[70] Struben, J., and Sterman, J. D., 2008, "Transition Challenges for Alternative Fuel Vehicle and Transportation Systems," Environ. Plan. B: Plan. Des., **35**(6), pp. 1070–1097.
[71] Moura, S. J., Callaway, D. S., Fathy, H. K., and Stein, J. L., 2008, "Impact of Battery Sizing on Stochastic Optimal Power Management in Plug-in Hybrid Electric Vehicles," IEEE International Conference on Vehicular Electronics and Safety, 2008, Columbus, OH, Sept. 22–24.